Effects of microstructure on flux pinning in epitaxial $YBa_2Cu_3O_x$ films

D. H. Kim, D. J. Miller, J. C. Smith, and R. A. Holoboff
Materials Science Division, Argonne National Laboratory, Argonne, Illinois 60439

J. H. Kang and J. Talvacchio
Westinghouse Science and Technology Center, Pittsburgh, Pennsylvania 15235
(Received 6 May 1991)

The role of microstructure on flux pinning in *c*-axis-oriented epitaxial $YBa_2Cu_3O_x$ films grown on $LaAlO_3$ and $SrTiO_3$ has been studied. For a magnetic field parallel to the Cu-O planes, the resistivity and critical current density J_c have been measured as a function of the angle θ between the applied field and the direction of the transport current. In addition to a Lorentz-force-independent resistivity, the Lorentz-force-dependent component showed several broad deviations from $\sin^2\theta$ when a field was aligned parallel to certain microstructural features which vary with the film thickness and substrate material. These features were identified by transmission-electron-microscopy analysis. For films of 5000 Å thickness on $LaAlO_3$, resistivity dips were observed for a field applied parallel to the *substrate* twin boundaries or along misoriented *a*-axis grains. In thinner films of 900 Å thickness also on $LaA1O_3$ in which *a*-axis grains were negligible, we observed dips corresponding to the orientation of *substrate* twin boundaries only. For thin films on $SrTiO_3$ in which substrate twins are absent, resistivity dips corresponding to the direction of twin boundaries in the *film* and, perhaps, interfacial dislocations were observed. Overall, such dips decreased with increasing transport current density and became negligible in J_c measurements.

I. INTRODUCTION

High-temperature superconductors (HTS's) exhibit unusually large magnetic-field-induced broadening of their resistive transitions, which generally increase with the anisotropy.[1-3] With the applied field **H** *parallel* to the superconducting Cu-O layers ($\mathbf{H}\|a$), the broadening is not as large due to the anticipated intrinsic pinning of the insulating (or normal) region between layers.[4,5] In highly anisotropic HTS's, such as $Bi_2Sr_2CaCu_2O_x$ (Ref. 6) and $Tl_2Ba_2CaCu_2O_x$ (Refs. 2,7), Lorentz-force-independent resistive transitions were observed and an explanation other than flux motion has been proposed.[7] However, for less anisotropic $YBa_2Cu_3O_x$, intrinsic pinning is smaller due to the shorter interlayer spacing and the conducting Cu-O chains between superconducting Cu-O double layers. In this material, a Lorentz-force-induced flux flow resistivity which varies as $\sin^2\theta$ has been observed in high-quality single crystals,[8] where θ is the angle between the direction of the transport current and magnetic field. Moreover, when a magnetic field is aligned parallel to the twin boundaries, a sharp drop in resistivity was found at the foot of the transition, indicating substantial flux pinning by twin boundaries.[8] Magnetization measurements also show a similar effect of flux pinning by twin boundaries.[9,10] A larger magnetization-hysteresis loop was observed for fields parallel to twin boundaries than perpendicular to the boundaries.[9] In thin films, flux pinning is more complex mainly due to the presence of the substrates. Iye *et al.*[11,12] measured the angular-dependent resistivity in epitaxial $YBa_2Cu_3O_x$ films and observed four broad dips which were attributed to the Lorentz-force effect and the *ab*-plane anisotropy averaged over twin domains.

In this paper, angular-dependent transport studies of high-quality epitaxial $YBa_2Cu_3O_x$ films are reported. Resistivity and critical-current density for $\mathbf{H}\|a$ as a function of angle θ were measured. Several dips are observed in the angular-dependent flux flow resistivity. In order to clarify the origins of the deviation from flux flow resistivity, transmission electron microscopy (TEM) was performed on samples prepared from the same batch. The relative orientations of the microstrip as well as various microstructural features with respect to the substrate were determined by TEM and electron diffraction to correlate with the angle θ between current and field at which the dips in resistivity were observed. Several dips were observed similar to the previous works of Iye *et al.*,[11,12] but we interpret the origin of dips as a pinning effect due to the microstructure in the films based on TEM rather than due to the *ab*-plane anisotropy. For films of 5000 Å thickness on $LaAlO_3$, four resistivity dips were observed in one period for a field applied parallel to substrate twin boundaries or along misoriented *a*-axis grains. In thinner films of 900 Å thickness also on $LaAlO_3$ in which *a*-axis grains were negligible, we observed only two dips, corresponding to the orientation of substrate twin boundaries. For thin films on $SrTiO_3$ in which substrate twins are absent, resistivity dips corresponding to the direction of twin boundaries in the film and, perhaps, interfacial dislocations were observed. Such pinning effects became weaker as the temperature or transport current was increased.

II. EXPERIMENT

Films on $YBa_2Cu_3O_x$ were grown *in situ* by dc magnetron sputtering from a stoichiometric target onto $LaAlO_3$ (100) and $SrTiO_3$ (100) substrates. TEM showed that films are epitaxial and *c*-axis oriented. All of the films studied here exhibit vanishing zero-field resistance around $T_c = 88-89$ K. The samples were patterned to form a 6–25 μm wide strip with conventional photolithography and ion milling. Gold was sputtered on the current and voltage pads to reduce the contact resistance. The typical distance between the voltage probes was 0.1 cm, thus we are measuring an averaged effect of the microstructures. Samples are placed in the rotating holder so that we can vary the angle θ with 1° resolution in the *ab* plane. At every θ position, samples are tilted back and forth slightly in the *ac* plane to find the minimum resistance. In this manner, the angular resolution achieved for the *ac* plane is much better than the full width at half maximum of the rocking curve (0.4°–0.5°).

Conventional techniques were used to prepare planar and cross-section samples for TEM. After grinding and dimpling, the samples were ion milled using 4 kV Ar with a low beam current while maintaining at liquid nitrogen temperatures to minimize damage to the films. The samples were imaged in a Philips CM-30 operating at either 100 or 300 kV. Among five samples of $YBa_2Cu_3O_x$ films studied, the characteristics of three representative films are listed in Table I. The other two showed almost identical behavior to samples 2 and 3.

III. RESULTS AND DISCUSSION

Figure 1 shows the resistive transition of a 5000 Å $YBa_2Cu_3O_x$ film on $LaAlO_3$ in zero field and 4 T for fields parallel to the current (**H**||**I**) and for fields perpendicular to the current (**H**⊥**I**). The inset shows the same transition plotted on a semilogarithmic scale. A slight double transition in zero field was usually observed in all samples grown on $LaAlO_3$ substrates but vanishes in finite fields (> 1 T). The Lorentz-force-dependent component is clearly observed in the 4 T field with a large Lorentz-force-independent background. This background broadening could be due to a mechanism other than flux-flow-induced dissipation[7,13] and is subject to future study. In this work, only the Lorentz-force-dependent part will be considered.

The angular-dependent resistivity at 90.5 K and 4 T with a measuring current density of 80 A/cm^2 is shown as circles in Fig. 2(a). A simple flux flow model predicts a $\sin^2\theta$ dependence with a maximum resistivity at **H**⊥**I**, shown as a solid line in Fig. 2(a), but data show additional four dips separated by 45° in one period. Deviation from an ideal flux flow resistivity, $\Delta\rho_{ff}$, is also plotted in Fig. 2(a) (diamonds) and four dips are seen more clearly. At a lower temperature, 87.9 K, the magnitudes of the dips increases [Fig. 2(b)] but a large transport current density of 8000 A/cm^2 significantly reduces the magnitude as shown in Fig. 2(c). This temperature- and current-dependent behavior suggests that the resistivity drop is due to the flux pinning effect. Such dips are no longer observable in J_c measurements [Fig. 2(d)], but a slight asymmetry is observed which is reminiscent of the dips. It is worthwhile to note that a similar J_c measurement in the low-T_c material[14] showed an in-plane anisotropy of greater than 20 with a $\sin^{-1}\theta$ dependence except near $\theta = 0°$, consistent with the Lorentz-force-induced dissipation. In this work, J_c anisotropy was found to be about 3 or less, considerably smaller than that in Ref. 14, and it decreased slightly at low temperatures and fields. In addition, a $\sin^{-1}\theta$ dependence was observed only near $\theta \approx 90°$. This behavior suggests that a mechanism other than flux-flow-induced dissipation limits J_c over a substantial region around $\theta \approx 0°$.

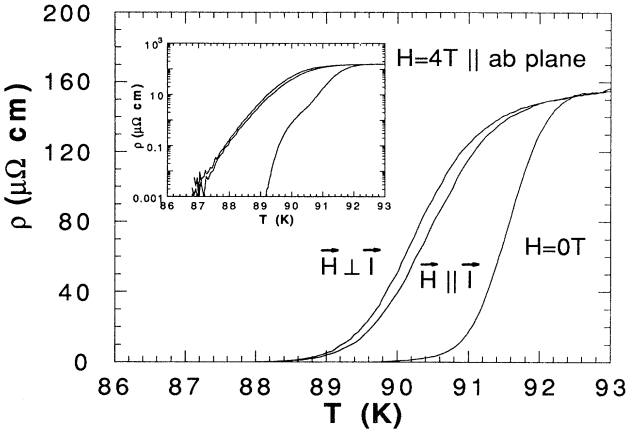

FIG. 1. Resistive transitions of sample 1 in 0 and 4 T fields are shown for **H**⊥**I** and **H**||**I**. A small Lorentz-force-dependent component with a large background broadening can be seen. Inset shows the same transition on a semilogarithmic scale.

TABLE I. The characteristics of the three representative $YBa_2Cu_3O_x$ films are listed. J_c was determined using a 2 μV/cm criterion. Samples 2 and 3 were grown from the same batch.

Sample	Substrate	Thickness (Å)	Width of strip (μm)	T_c (K)	J_c at 77 K and 0 T (A/cm^2)
1	$LaAlO_3$(100)	5000	25	89.2	1.0×10^6
2	$LaAlO_3$(100)	900	13	87.8	2.3×10^6
3	$SrTiO_3$(100)	900	6	89.4	4.1×10^6

A typical TEM micrograph of a planar section of sample 1 is shown in Fig. 3(a). Needle-shaped crystallites marked A are *a*-axis-oriented grains, while larger particles marked *B* are CuO, as identified by EDS and electron diffraction. Figure 3(b) shows a higher magnification image of a misoriented grain in which *c*-axis fringes can be clearly seen. Electron diffraction showed that these particles are oriented along either *a* or *b* axis of the *c*-axis-oriented background, so that these grains are aligned with the principal axes of the substrate. Epitaxial formation at the substrate and film boundaries can be seen in Fig. 4(a) in the cross-sectional TEM micrograph. The *a*-

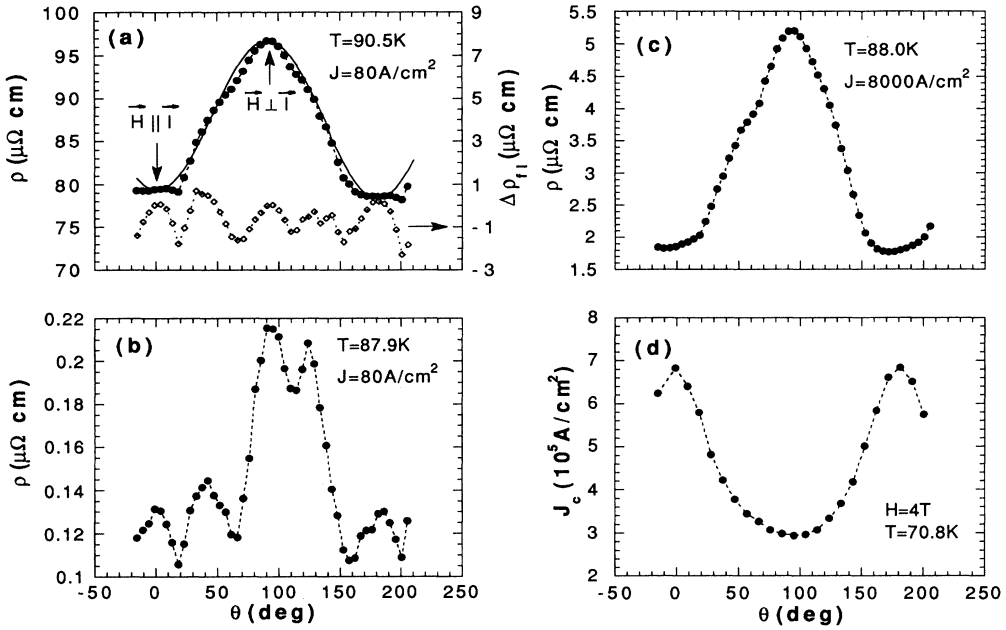

FIG. 2. (a) Angular-dependent resistivity of sample 1 at 90.5 K and 4 T with a measuring current density of 80 A/cm^2 is shown as circles. Solid lines are a $\sin^2\theta$ fit and dotted lines are a guide to the eye. Deviation from ideal flux flow resistivity, $\Delta\rho_{fl}$, is also plotted as diamonds and four dips separated by 45° are clearly seen. (b) Resistivity dips develop sharply at 87.9 K. Field and measuring current density are the same as (a). (c) At the same condition as (b), but a large transport current density of 8000 A/cm^2 reduces the magnitude of the dips. (d) The J_c measurement at 70.8 K shows hardly any dip.

axis grains nucleate only beyond a certain film thickness of the order of a few hundred angstroms, not directly from the substrate as shown in Fig. 4(b).

$LaAlO_3$ substrates become heavily twinned during the cool-down process after the *in situ* growth of films and these twin boundaries are oriented 45° from the principal axis, thus any twin boundaries in $YBa_2Cu_3O_x$ films would be parallel to the substrate twin boundaries. However, it was not clear whether this film is twinned or not. In some plane-section images, evidence of twinning is observed, but selected area diffraction patterns do not show the typical spot splitting associated with twins in $YBa_2Cu_3O_x$. Additionally, the structure resembling twins is observed only when the underlying substrate is also present. In regions that have been thinned so that no substrate remains, this twin structure is absent. One might argue that the absence of twins in the free-standing part of the film is due to untwinning during sample preparation such as ion milling, but the samples were kept at 77 K during ion milling so that the resulting local heating is not sufficient enough to untwin the film. Similarly prepared specimen of the single crystals and films on $SrTiO_3$ showed no such untwinning effect. Thus, it is considered that this film is free of twins, but that the presence of substrate twins induces a change in the direction of strain associated with the slight misfit between $YBa_2Cu_3O_x$ and $LaAlO_3$.

There is a correlation between the orientation of each of the microstructural features with resistivity drops. The relatively broader dips at 65° and 155° in Fig. 2 correspond to the substrate twin boundary orientations. The resistivity drop for a field parallel to the substrate twin boundaries may be due to flux pinning by undetermined microstructural features in the sample induced by strain associated with the substrate twins. The other dips at 20° and 110° correspond to the directions along the needle shape of the *a*-axis-oriented particles. There are two possibilities for these two dips: flux pinning at the boundaries between the misoriented crystal and the background material or the resistivity anisotropy between $\mathbf{H}\|c$ and $\mathbf{H}\|a$ of the *a*-axis grains. In the latter case, the resistivity contribution from the *a*-axis grain is minimum when the field is aligned parallel to the Cu-O planes of the *a*-axis grains. Then the magnitude of the dip should be roughly the product of the volume occupied by *a*-axis grains and the resistivity difference between $\mathbf{H}\|c$ and $\mathbf{H}\|a$. The volume of *a*-axis grains was estimated from TEM micrographs and the resistivity difference at the corresponding temperatures was measured. It was found that about 30% of the resistivity drop can be accounted for on this basis. This suggests that other mechanism of pinning, perhaps due to a *a*-axis grain boundaries or some other features, are dominant.

Iye *et al.*[11,12] explained the dips for the field along the *a* or *b* axis (in this case, along the *a*-axis grains) as a result of the *ab*-plane anisotropy averaged over twin domains. However, the measurements on the twinned single crystals[8] did not show any dips associated with the *ab*-plane anisotropy, and recent magnetic measurements on the *untwinned* single crystals showed no significant *ab*-plane anisotropy in the lower[15] and upper critical fields.[16] The *ab*-plane resistivity anisotropy of the untwinned single crystals for magnetic fields parallel to the Cu-O planes has not been reported to our knowledge.

Since the *a*-axis-oriented grains start to grow only beyond a certain film thickness [Fig. 4(b)], the effect of the misoriented grains can be reduced by growing thinner films. The resistive transitions for a 900-Å-thick film on $LaAlO_3$ (sample 2) in 0 and 4 T fields for $\mathbf{H}\|\mathbf{I}$ and $\mathbf{H}\perp\mathbf{I}$ are shown in Fig. 5 on a linear and logarithmic scale. Measurements of resistivity as a function of angle θ at 88.0 K display an ideal flux flow resistivity as shown in Fig. 6(a) for a measuring current density of 160 A/cm^2. This temperature is approximately equivalent to 90.5 K in the thicker film of sample 1 where resistivity dips due to microstructural features were observed. It implies that defect structures, such as *a*-axis-oriented grains, grow with film thickness and so does the pinning effect. At a lower temperature, 86.7 K, only *two* dips at 53° and 143° corresponding to the orientation of the substrate twin boundaries are evident as shown in Fig. 6(b). The dips resulting from the misoriented particles are negligible as expected. This result is consistent with the absence of *a*-axis grains as confirmed by TEM of a film cross section. Similar measurements on a 1500-Å-thick film on $LaAlO_3$ also showed only two dips corresponding to *a*-axis grains. At higher transport current densities, reduction of the dips has been observed similar to the case of sample 1, and the critical-current density at 77 K showed no dips at all. This behavior suggests that these microscopic structures are not effective pinning centers for high current applications, and more uniformly distributed pinning centers, such as oxygen vacancies and dislocations, could be more effective at low temperatures.

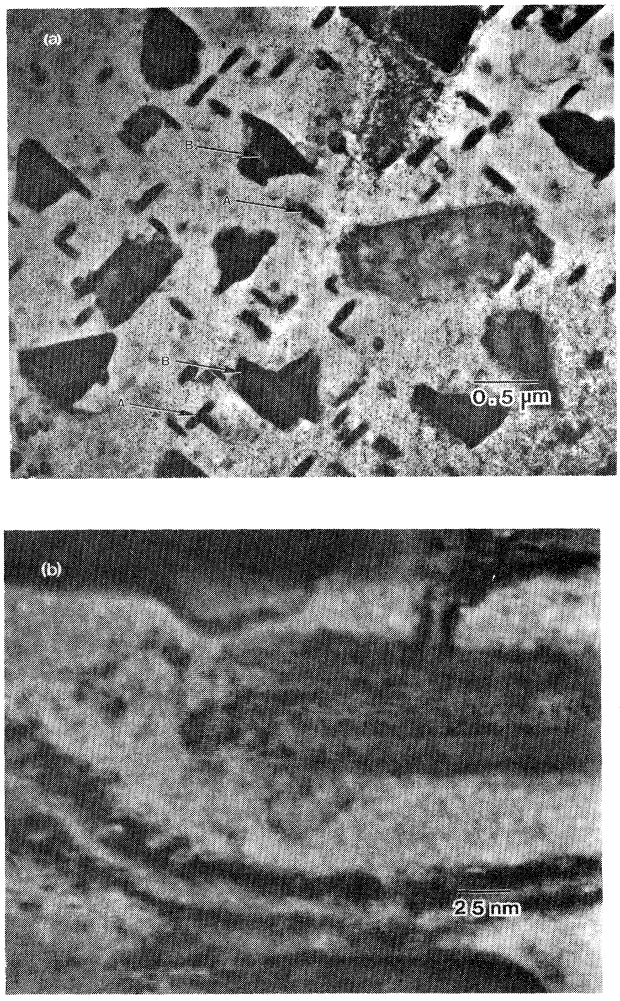

FIG. 3. (a) Bright-field electron micrograph of a planar section of $YBa_2Cu_3O_x$ on $LaAlO_3$. The needle-shaped crystallites marked A are *a*-axis-oriented grains, and the larger particles marked B are CuO. (b) Higher magnification image of the same plane section showing an *a*-axis-oriented particle. Electron diffraction pattern shows the *c* axis of this particle to be parallel to the *a* or *b* axis of the matrix grain.

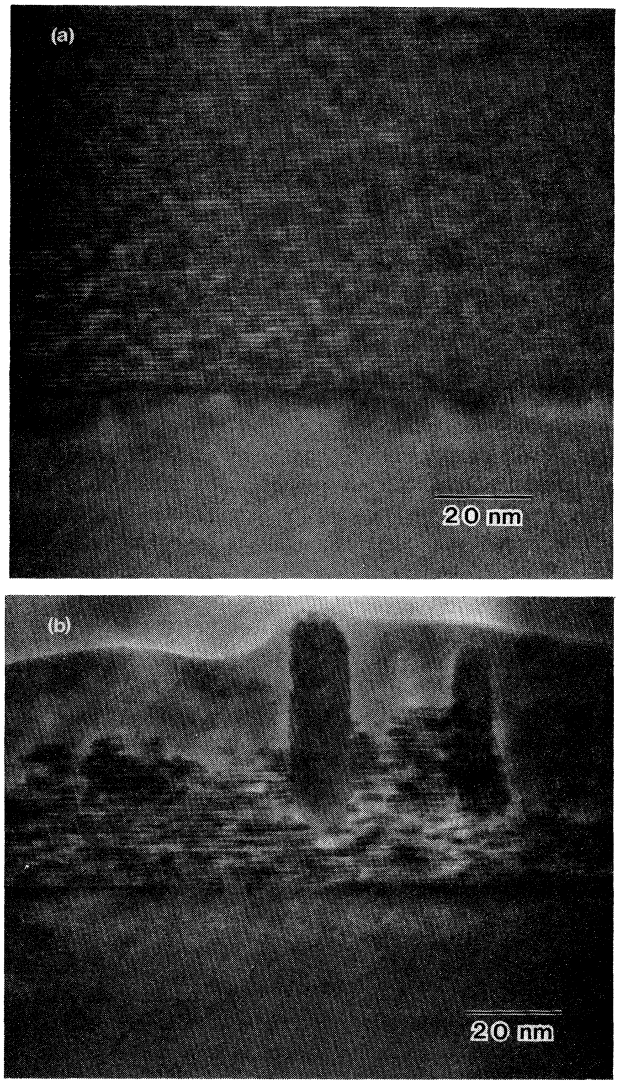

FIG. 4. (a) Bright-field electron micrograph of a cross section of the film showing epitaxial growth of a film near the substrate. (b) Low magnification image of the cross section showing *a*-axis grains which nucleate only when the film has reached a minimum thickness.

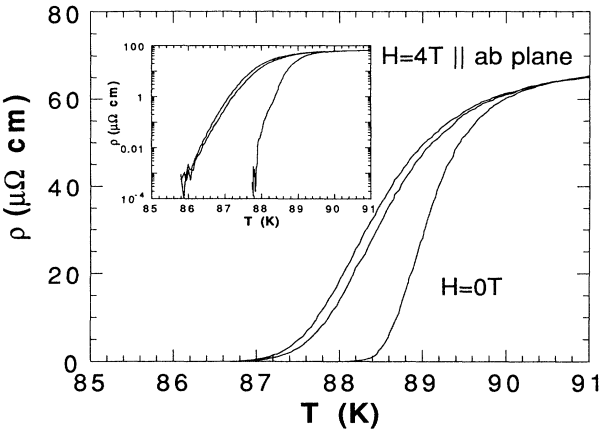

FIG. 5. Resistive transitions of sample 2 in 0 and 4 T fields are shown for **H⊥I** and **H||I**.

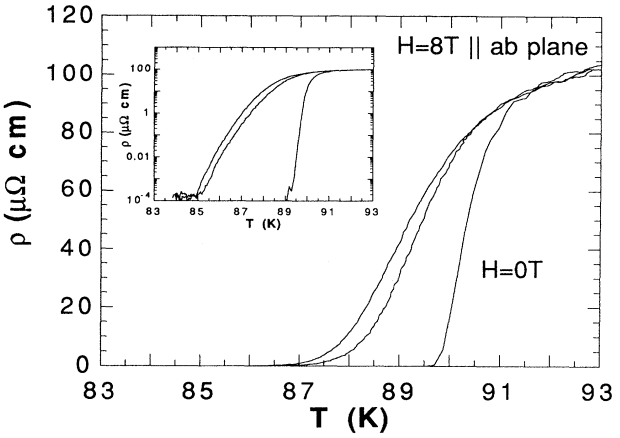

FIG. 7. Resistive transitions of sample 3 in 0 and 8 T fields are shown for **H⊥I** and **H||I**.

So far, the discussion has been limited to samples grown on $LaAlO_3$ where *substrate* twin boundaries play an important role in flux pinning for small transport currents (typically $J < 10^4$ A/cm^2). On the other hand, $SrTiO_3$ does not form any twin structure, thus it is interesting to study films grown on this substrate for comparison. We have measured two samples on $SrTiO_3$ from the same batch as sample 2, and they exhibit almost identical behavior. Figure 7 shows resistive transitions in 0 and 8 T fields for sample 3 of 900 Å thickness.

The angular dependence of the resistivity at 88.3 K for 8 T with a measuring current density of 270 A/cm^2 is shown in Fig. 8(a), and an ideal flux flow resistivity is observed. At 86.3 K, three dips develop in one period as shown in Fig. 8(b). At higher transport current densities, reduction of the dips has been observed, similar to the case of samples 1 and 2. The critical-current density at low temperatures showed no structure at all. The TEM plane section (Fig. 9) shows twin boundaries in the sample, and electron diffraction indicates that the twin boun-

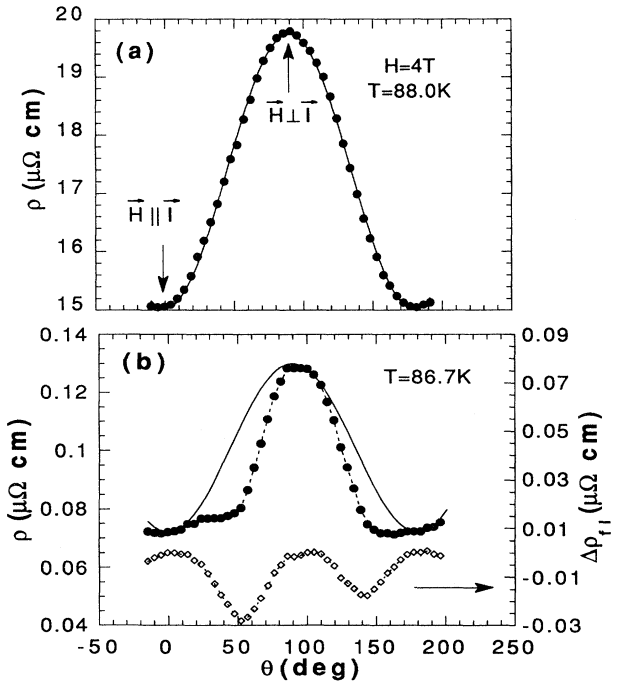

FIG. 6. Angular-dependent resistivities of sample 2 at (a) 88.0 K and (b) 86.7 K for a 4 T field with a measuring current density of 160 A/cm^2 are shown as circles. Ideal flux flow resistivity was observed at 88.0 K. At 86.7 K, two dips separated by 90° were observed. $\Delta\rho_{fl}$ are plotted as diamonds in (b).

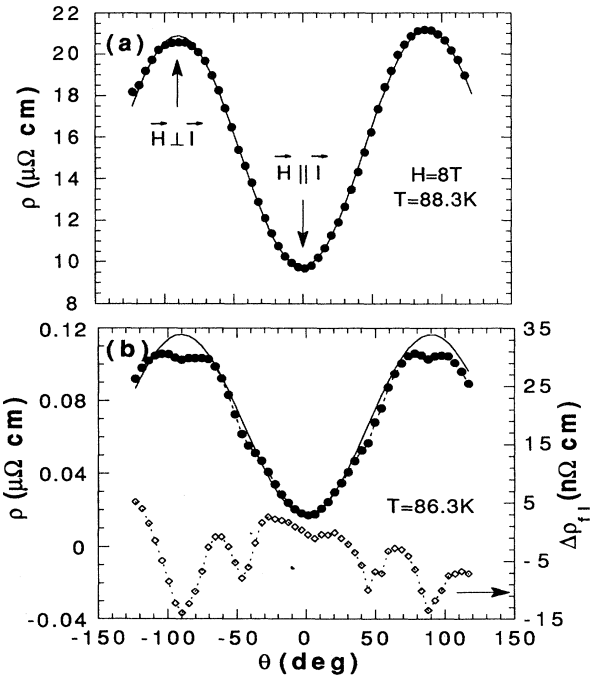

FIG. 8. Angular-dependent resistivities of sample 3 at (a) 88.3 K and (b) 86.3 K for an 8 T field with a measuring current density of 270 A/cm^2 are shown as circles. Ideal flux flow resistivity was observed at 88.3 K. At 86.7 K, three dips were observed in one period. $\Delta\rho_{fl}$ are plotted as diamonds in (b).

daries are along the [110] direction of the $SrTiO_3$, which is expected to be due to the epitaxial relationship between $YBa_2Cu_3O_x$ and $SrTiO_3$. Since the microstrip is patterned along the [100] direction of the substrates, the dips at $\pm 45°$ correspond to the twin boundary direction of the film. The resistivity drop may be due to the twin boundary pinning effect. The relatively broad dips compared to those of the single-crystal work[8] suggest that the orientations of the twin boundaries throughout the sample have a certain angular distribution ($\sim \pm 10°$), but strain associated with the slight misfit between $YBa_2Cu_3O_x$ and $SrTiO_3$ could be responsible for the broader dips.

It is interesting to note that the relative resistivity drops due to the twin boundaries in the films are noticeably smaller and narrower than the corresponding drops at the same angular positions in sample 2 on $LaAlO_3$ grown from the same batch. This suggests that the effects of certain microstructural features induced by the substrate twins are dominant over the pinning effect of the intrinsic twin boundaries in $YBa_2Cu_3O_x$ thin films.

The dips at $\pm 90°$ could be due to *a*-axis-oriented grains. Although no evidence of *a*-axis grains was observed in TEM cross sections, plane-section TEM revealed very small *a*-axis grains, and some of these are indicated by arrows in Fig. 9. Since these grains are quite small (≈ 100 Å), the overall effective volumes or surfaces are negligible. Furthermore, the effect of these grains was negligible in transport measurements of sample 2 from the same batch. Another possible origin of these dips could be the flux pinning along dislocations. A high density of interfacial dislocations typically oriented along the [100] and [010] directions of $SrTiO_3$ was observed. The dislocations were observed to be unique to films grown on $SrTiO_3$. However, we do not have further evidence to directly correlate the dips at $\pm 90°$ to the flux pinning at the dislocations. Both of these mechanisms predict a dip at every 90°, so a dip is expected at 0°. However, because the macroscopic Lorentz force vanishes for $\mathbf{H} \| \mathbf{I}$, no such dips are observable except a small glitch at 0°.

Finally, the double transition observed in films on $LaAlO_3$ in small fields (< 1 T) indicates a T_c variation in the sample, and it is very likely that a part of the film along the substrate twin boundaries may have a different T_c from the rest of the film due to the induced microstructural features. The absence of the double transition in films on $SrTiO_3$ is consistent with this speculation. A detailed study of the influence of the substrate twin boundaries of $LaAlO_3$ on the microstructures is under way.

IV. SUMMARY

We have measured resistivity and critical-current density as a function of angle between the applied field and the direction of transport current for fields parallel to the Cu-O layers in high-quality epitaxial $YBa_2Cu_3O_x$ films. Several dips were observed in the angular-dependent flux

FIG. 9. Bright-field electron micrograph of a planar section of $YBa_2Cu_3O_x$ on $SrTiO_3$ showing a twinned structure. Some *a*-axis grains are indicated by arrows.

flow resistivity. TEM samples were prepared to investigate the origins of the deviation from flux flow resistivity. For thick films (5000 Å) on $LaAlO_3$, resistivity dips are observed when a field is aligned parallel to *substrate* twin boundaries or along the *a*-axis grains. In thinner films (900 Å) in which *a*-axis grains were negligible, only two dips were observed, corresponding to the orientation of substrate twin boundaries. The resistivity drop for a field parallel to the substrate twin boundary may be due to flux pinning by undetermined microstructural features in the sample induced by strain associated with the substrate twins. For fields along the *a*-axis grains, flux pinning at the grain boundaries and/or resistivity anisotropy between $\mathbf{H}\|c$ and $\mathbf{H}\|a$ can be responsible for resistivity dips.

Meanwhile, for films grown on $SrTiO_3$, twin structures in the film were observed in TEM, and the pinning effect due to the twin boundaries was also observed in the angular-dependent flux flow resistivity. In addition, a pinning effect due to the other microstructural features, perhaps interfacial dislocations, was observed in films grown on $SrTiO_3$. Overall, such pinning effects weaken as the transport current increases and become at most a perturbation in high-current applications.

ACKNOWLEDGMENTS

The authors thank J. Hettinger for valuable discussions and K. E. Gray for a critical reading of the manuscript. This work is partially supported by the U.S. Department of Energy, Division of Basic Energy Sciences-Materials Sciences (W-31-109-ENG-38), the National Science Foundation (DMR 88-09854) through the Science and Technology Center for Superconductivity, and the AFOSR (F49620-88-C-0043). JCS and RAH acknowledge support from the Argonne Division of Educational Programs.

[1]T. T. M. Palstra, B. Batlogg, L. F. Schneemeyer, and J. V. Waszczak, Phys. Rev. Lett. **61**, 1662 (1988); T. T. M. Palstra, B. Batlogg, R. B. van Dover, L. F. Schneemeyer, and J. V. Waszczak, Appl. Phys. Lett. **54**, 763 (1989).

[2]K. C. Woo, K. E. Gray, R. T. Kampwirth, J. H. Kang, S. J. Stein, R. East, and D. M. McKay, Phys. Rev. Lett. **63**, 1877 (1989).

[3]D. H. Kim, K. E. Gray, R. T. Kampwirth, J. C. Smith, D. S. Richeson, T. J. Marks, J. H. Kang, J. Talvacchio, and M. Eddy, Physica C **177**, 431 (1991).

[4]M. Tachiki and S. Takahashi, Solid State Commun. **70**, 291 (1989).

[5]D. Feinberg and C. Villard, Phys. Rev. Lett. **65**, 919 (1990).

[6]Y. Iye, S. Nakamura, and T. Tamegai, Physica C **159**, 433 (1989).

[7]D. H. Kim, K. E. Gray, R. T. Kampwirth, and D. M. McKay, Phys. Rev. B **42**, 6249 (1990).

[8]W. K. Kwok, U. Welp, G. W. Crabtree, K. G. Vandervoort, R. Hulscher, and J. Z. Liu, Phys. Rev. Lett. **64**, 966 (1990).

[9]J. Z. Liu, Y. X. Jia, R. N. Shelton, and M. J. Fluss, Phys. Rev. Lett. **66**, 1354 (1991).

[10]L. J. Swartzendruber, A. Roitrurd, D. L. Kaiser, F. W. Gayle, and L. H. Bennett, Phys. Rev. Lett. **64**, 483 (1990).

[11]Y. Iye, S. Nakamura, T. Tamegai, T. Terashima, K. Yamamoto, and Y. Bando, Physica C **166**, 62 (1990).

[12]Y. Iye, A. Watanabe, S. Nakamura, T. Tamegai, T. Terashima, K. Yamamoto, and Y. Bando, Physica C **167**, 278 (1990); Y. Iye, S. Nakamura, A. Watanabe, and T. Tamegai (unpublished).

[13]T. Tsuneto, J. Phys. Soc. Jpn. **57**, 3499 (1989).

[14]G. D. Cody and G. W. Cullen, RCA Rev. **25**, 466 (1964); J. W. Heaton and A. C. Rose-Innes, Cryogenics **4**, 85 (1964); V. R. Karasik and V. G. Veresshchagin, Zh. Eksp. Teor. Fiz. **59**, 36 (1970) [Sov. Phys. JETP **32**, 20 (1971)].

[15]A. Umezawa, G. W. Crabtree, U. Welp, W. K. Kwok, K. G. Vandervoort, and J. Z. Liu, Phys. Rev. B **42**, 8744 (1990).

[16]U. Welp, M. Grimsditch, H. You, W. K. Kwok, M. M. Fang, G. W. Crabtree, and J. Z. Liu, Physica C **161**, 1 (1989).

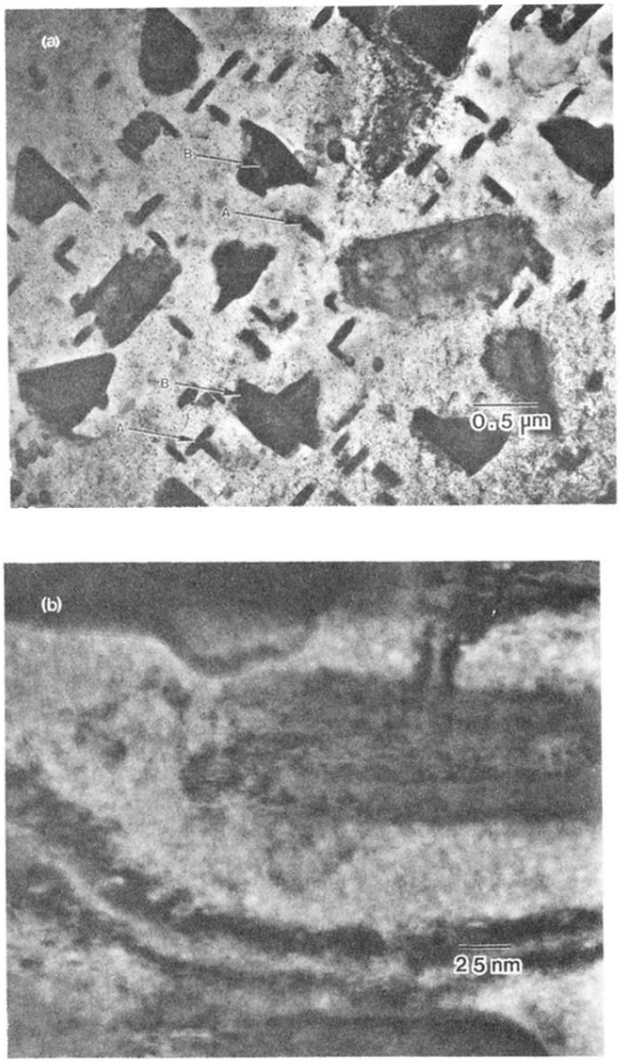

FIG. 3. (a) Bright-field electron micrograph of a planar section of $YBa_2Cu_3O_x$ on $LaAlO_3$. The needle-shaped crystallites marked A are *a*-axis-oriented grains, and the larger particles marked B are CuO. (b) Higher magnification image of the same plane section showing an *a*-axis-oriented particle. Electron diffraction pattern shows the *c* axis of this particle to be parallel to the *a* or *b* axis of the matrix grain.

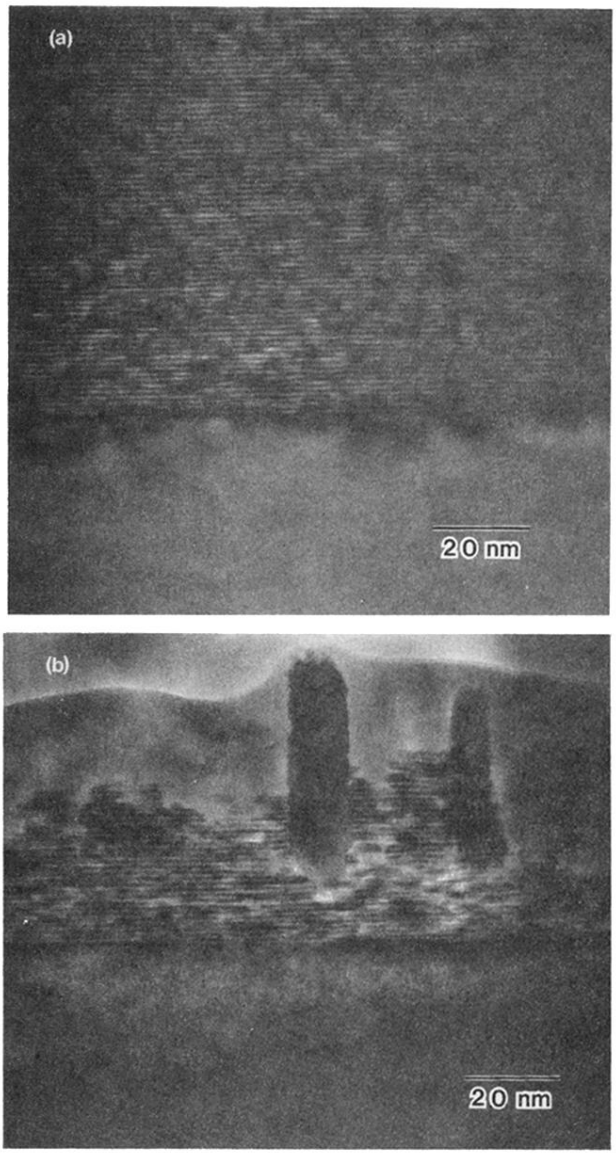

FIG. 4. (a) Bright-field electron micrograph of a cross section of the film showing epitaxial growth of a film near the substrate. (b) Low magnification image of the cross section showing *a*-axis grains which nucleate only when the film has reached a minimum thickness.

FIG. 9. Bright-field electron micrograph of a planar section of $YBa_2Cu_3O_x$ on $SrTiO_3$ showing a twinned structure. Some *a*-axis grains are indicated by arrows.